creased. The rate can also be increased if polar compounds are used as modifiers. The use of THF as a modifier also reduces the induction period usually associated with heterogeneous initiators, such as lithium morpholinide. The increase in copolymerization rate and decrease in induction period are believed to be related to a change from a heterogeneous to homogeneous polymerization upon dissolution of the initiator. Other additives, such as DPE, TMEDA, NEt_3, and glyme, do not reduce the induction period at the ratio 0.031:1 lithium morpholinide to modifier. These systems remain heterogeneous in nature. However, it is expected that the induction period would be eliminated if additional amounts of modifier were used in this system.

Finally, we have found that the presence of oxygen as a built-in modifier in the lithium morpholinide initiator does not give a copolymer with unusual properties. No randomization of styrene was observed in the butadiene–styrene copolymerization. As a result, the copolymerization with lithium morpholinide behaves like the alkyllithium system.

Acknowledgment. The author thanks Mr. L. L. Wolf, who conducted the kinetic study, and Drs. D. N. Schulz and T. A. Antkowiak for discussions. The author also thanks the Firestone Tire & Rubber Co. for permission to publish this work.

References and Notes

(1) Antkowiak, T. A.; Oberster, A. E.; Halasa, A. F.; Tate, D. P. *J. Polym. Sci., Part A-1* **1972**, *10*, 1319.
(2) Zelinski, R. P. U.S. Patent 2975160, 1961.
(3) Kuntz, I. *J. Polym. Sci.* **1961**, *54*, 569.
(4) Hsieh, H. L.; Glaze, W. H. *Rubber Chem. Technol.* **1970**, *43*, 22.
(5) Cheng, T. C. *Polym. Prepr., Am. Chem. Soc., Div. Polym. Chem.* **1980**, *21* (1), 30.
(6) Kern, W. J.; Anderson, J. N.; Adams, H. E.; Bouton, T. C.; Bethea, T. W. *J. Appl. Polym. Sci.* **1972**, *16*, 3123.
(7) Korothor, A. A.; Chesnokova, N. N. *Vysokomol. Soedin.* **1960**, *2*, 365.
(8) Kelley, J. D.; Tokolsky, A. V. *J. Am. Chem. Soc.* **1959**, *81*, 1597.
(9) Kuntz, I.; Gerber, A. *J. Polym. Sci.* **1960**, *42*, 299.
(10) Stearns, R. S.; Forman, L. E. *J. Polym. Sci.* **1959**, *41*, 381.
(11) Szwarc, M. *J. Polym. Sci.* **1959**, *40*, 583.
(12) O'Driscoll, K. F.; Kuntz, I. *J. Polym. Sci.* **1962**, *61*, 19.
(13) Angood, A. C.; Hurley, S. A.; Tait, J. T. *J. Polym. Sci., Polym. Chem. Ed.* **1975**, *13*, 2437.
(14) Saltman, W. W. "The Stereo Rubbers"; Wiley: New York, 1977; Chapter 5, pp 215–84.
(15) Oliver, J. P.; Smart, J. B.; Emerson, M. T. *J. Am. Chem. Soc.* **1966**, *88*, 4101.
(16) Smart, J. P; Hogan, R.; Scherr, P. A.; Emerson, E. T.; Oliver, J. P. *J. Organomet. Chem.* **1974**, *64*, 1.
(17) Glaze, W. H.; Hanicak, J. E.; Moore, M. L.; Chandhuri, J. *J. Organomet. Chem.* **1972**, *44*, 39.
(18) Morton, M. *High Polym.* **1964**, *18*, 421.
(19) Korotkov, A. A. *Int. Symp. Macromol. Chem., Prague, Sept 1957*, paper no. 66.
(20) Morton, M.; Ells, F. R. *J. Polym. Sci.* **1962**, *61*.
(21) Johnson, A. F.; Worsfold, D. J. *Makromol. Chem.* **1965**, *85*, 273.
(22) Hsieh, H. L. *J. Polym. Sci., Part A* **1965**, *3*, 181.
(23) Cheng, T. C., unpublished results.
(24) Turner, R. R.; Altenau, A. G.; Cheng, T. C. *Anal. Chem.* **1970**, *42*, 1835.
(25) Binder, J. L. *Anal. Chem.* **1954**, *26*, 1877.
(26) Binder, J. L. *J. Polym. Sci., Part A* **1963**, *1*, 47.
(27) Mochel, V. D. *Rubber Chem. Technol.* **1967**, *40*, 1200.

Thermodynamic Properties of Moderately Concentrated Solutions of Linear Polymers†

Ichiro Noda,* Narundo Kato, Toshiaki Kitano, and Mitsuru Nagasawa

Department of Synthetic Chemistry, Nagoya University, Furō-chō, Chikusa-ku, Nagoya 464, Japan. *Received January 30, 1980*

ABSTRACT: The osmotic pressure, light scattering, and vapor pressure of linear polymer solutions in the moderately concentrated region were studied for poly(α-methylstyrenes) having sharp molecular weight distributions and covering a wide range of molecular weight. The reduced osmotic pressure $\pi M/CRT$, where M is the molecular weight and C is the polymer concentration, was found to be a universal function of the degree of coil overlapping, which is defined by the ratio of polymer concentration C to a critical concentration C^*. In moderately concentrated solution, where C is larger than C^*, $\pi M/CRT$ is proportional to $(C/C^*)^{1.32_5}$, in good agreement with the scaling theory of des Cloizeaux.

Introduction

Many papers have been published to show that the thermodynamic and viscoelastic properties of linear polymer solutions show different behavior in three concentration regions. In dilute solutions, the thermodynamic properties are determined by the excluded-volume effect working between segments, and polymer coils in good solvents may be approximately regarded as hard spheres with respect to intermolecular interactions.[1,2] Many theoretical and experimental works have been published on the thermodynamic properties of dilute solutions. In concentrated solutions, polymer coils overlap so extensively that the excluded-volume effect of polymer coils disappears and the segments are uniformly distributed over the solution.[3] The thermodynamic properties of concentrated solutions are well explained on the basis of the theory of Flory and Huggins.[3]

In the intermediate region, that is, in moderately concentrated solution, the polymer coils partially interpenetrate each other, so that the thermodynamic properties may be different from either dilute or concentrated solutions. The thermodynamic properties of moderately concentrated solutions have not extensively been studied in comparison with those of dilute and concentrated solutions. It is important to study the thermodynamic properties of moderately concentrated solutions not only because it is interesting to examine how the excluded volume is affected by coil overlapping but also because moderately

†Presented in part at the 26th International Congress of Pure and Applied Chemistry, Tokyo, Japan, Sept 1977.

0024-9297/81/2214-0668$01.25/0

Table I
Characteristics of Poly(α-methylstyrenes)

sample no.	$\bar{M}_n \times 10^{-4}$	$\bar{M}_w \times 10^{-4}$	$\bar{M}_w/\bar{M}_n$	$\langle s^2\rangle \times 10^{-4}$,[a] Å^2	$C^* \times 10^2$, g/cm^3	$V_2^* \times 10^2$
α-104	7.08			0.84[b]	3.6_4	3.0_5
α-12	20.0	20.4	1.02	3.18	1.40	1.17
α-103	50.6			8.4[b]	0.82_3	0.69
α-110	119	119	1.00	23.0	0.42_8	0.35_8
α-112		182		39.7	0.288	0.251
α-113		330		73.3	0.209	0.175
α-111		747		187	0.116	0.097

[a] In toluene at 25 °C. [b] Calculated by eq 24.

concentrated solutions are important in other fields of study.[4]

To discuss the thermodynamic properties of flexible polymers, therefore, it appears convenient to classify the polymer solutions according to the degree of coil overlapping, which is defined by the ratio of the polymer concentration to the critical concentration (C^*) where polymer coils begin to overlap each other. C^* is defined by

$$C^* = M/(4/3)\pi\langle s^2\rangle^{3/2}N_A \quad (1)$$

where N_A is Avogadro's number and M and $\langle s^2\rangle^{1/2}$ are the molecular weight and radius of gyration of the polymer, respectively. Since the volume fraction of polymers, v_2, is the product of the weight concentration C and the specific volume $\bar{v}$ of the polymer, i.e., $v_2 = C\bar{v}$, C^* is also related to the critical volume fraction v_2^* by $v_2^* = C^*\bar{v}$. Thus, polymer solutions may be classified into three different concentration regions with respect to the critical volume fraction v_2^*, that is, dilute ($v_2 \ll v_2^*$), moderately concentrated ($v_2^* \ll v_2 \ll 1$) and concentrated ($v_2 \sim 1$) solutions.

Since the degree of coil overlapping depends on both concentration and dimension of polymer coil, it is important to study the molecular weight dependence of the thermodynamic properties of polymer solution at finite concentrations. In the present work, we measure osmotic pressure, light scattering, and vapor pressure of nearly monodisperse poly(α-methylstyrenes) in toluene at 25 °C over wide ranges of molecular weight and concentration.

Experimental Section

Materials. The samples used here are the same poly(α-methylstyrenes) having sharp molecular weight distributions as used in previous studies.[1,2,5,6] Their molecular characteristics are shown in Table I. The molecular weight ranges from ca. 7×10^4 to 7×10^6. The critical concentration calculated from eq 1 ranges from about 3 to 0.1% as shown in Table I. Toluene, which is a good solvent for the present sample, was purified by the same method as reported previously.[1]

Osmotic Pressure Measurements. Three types of osmometers were used for measurements of osmotic pressure since the measurements were carried out in a wide range of concentration: a Flory–Daoust osmometer (FD),[7] a modified Zimm–Myerson osmometer (ZM),[8] and a Hewlett-Packard Type 502 high-speed membrane osmometer (HM). The membrane used in the FD and ZM osmometers was a gel cellophane and the membrane for the HM osmometer was a Type S&S 0-8. The membrane conditioning was carried out by successively using mixtures of water–ethanol and ethanol–toluene. The osmotic pressure measurements in dilute solutions were carried out by using the HM osmometer as well as by a static method using the ZM osmometer, while the measurements in moderately concentrated solutions were carried out by using the HM osmometer as well as by a dynamic method[9] using the ZM and FD osmometers. An external pressure was applied to balance the osmotic pressure if necessary. All measurements were carried out at 25 °C.

Light Scattering Measurements. The light scattering measurements were carried out with a modified Shimadzu light scattering photometer at 25 °C. An unpolarized light of 436 nm was used as an incident beam. The solvent and solutions were filtered directly into the cell through Millipore filters of 0.45- and 1-μm pore size.

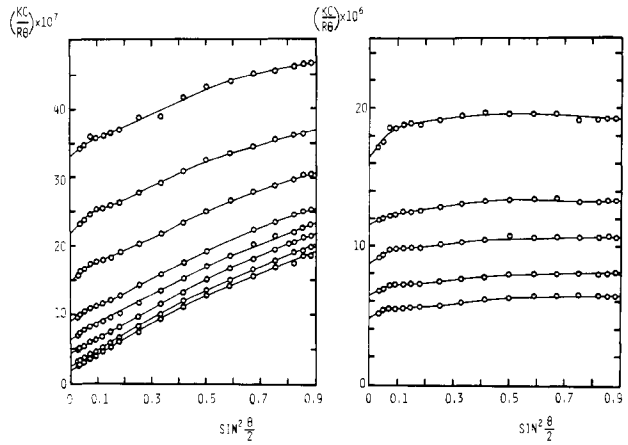

Figure 1. Angular dependence of light scattering from poly(α-methylstyrene) α-111 in toluene at 25 °C. The curves on the left side denote data at concentrations of 0.033_5, 0.052_4, 0.097_0, 0.142_7, 0.194_5, 0.288_1, 0.391_3, and 0.530_8 g/dL from bottom to top and the curves on the right side denote data at concentrations of 0.744_6, 0.932_6, 1.203, 1.448, and 1.956 g/dL from bottom to top.

The reduced intensity of light scattered from a polymer solution at a weight concentration C is given by

$$\frac{KC}{R_\theta} = \frac{1}{\bar{M}_w P(u)} + 2A_2[P_2(u)/P^2(u)]C + \ldots \quad (2)$$

with

$$u = \frac{16\pi^2}{\lambda'^2}\langle s^2\rangle \sin^2\frac{\theta}{2}$$

where K is the optical constant for light scattering, R_θ is the reduced intensity of scattered light at scattering angle θ, $\bar{M}_w$ is the weight-average molecular weight, λ' is the wavelength of incident light in the solution, $\langle s^2\rangle^{1/2}$ is the radius of gyration, and $P(u)$ and $P_2(u)$ are the particle scattering factors from one and two polymer molecules, respectively.

Examples of the angular dependence of scattered light at finite concentrations are shown in Figure 1. The limiting value at $\theta = 0$, $(KC/R_\theta)_{\theta=0}$, was obtained by a graphical extrapolation. The concentration dependence of $(KC/R_\theta)_{\theta=0}$ thus determined is shown in Figure 2.

At the limit of zero scattering angle the reduced intensity is related to the derivative of osmotic pressure with respect to concentration, $d\pi/dC$, as follows:[10]

$$\left(\frac{KC}{R_\theta}\right)_{\theta=0} = \frac{1}{RT}\frac{d\pi}{dC} \quad (3)$$

Using this relationship, we can evaluate the osmotic pressure π/C by

$$\pi/CRT = \frac{1}{C}\int_0^C \left(\frac{KC}{R_\theta}\right)_{\theta=0} dC \quad (4)$$

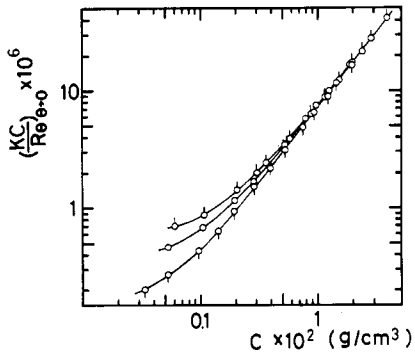

Figure 2. Concentration dependence of $(KC/R_\theta)_{\theta=0}$ for poly(α-methylstyrenes) in toluene at 25 °C. The symbols ◇, ○, and ▽ denote data for α-112, α-113, α-111, respectively.

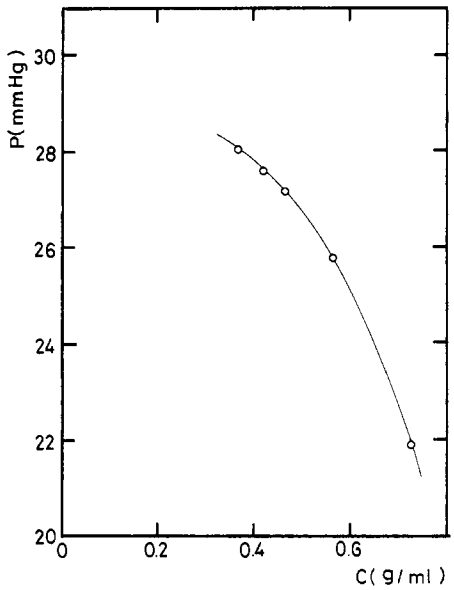

Figure 3. Concentration dependence of vapor pressure P for poly(α-methylstyrene) α-112 in toluene at 25 °C.

Vapor Pressure Measurements. Vapor pressures of concentrated solutions of the sample α-112 were measured by a gravimetric technique at 25 °C. Concentrations of polymer solutions were determined from the weight of polymer taken and the weight of solution measured by a quartz spring after the weight reached an equilibrium. The vapor pressure was changed by changing the temperature of the pure solvent reservoir. Equilibrium states were reached in 5 days. No hysteresis was observed. Figure 3 shows the equilibrium vapor pressure vs. concentration relationship for α-112.

The vapor pressure of solution, P, is related to π as

$$\pi V_1^\circ = -RT \ln (P/P_0) \tag{5}$$

where V_1° is the partial molar volume of the solvent and P_0 is the vapor pressure of the solvent.

Density Measurement. Density measurements were carried out with a Lipkin pycnometer of 25 mL at 25 °C to convert the weight concentration into volume fraction of polymer.

Results

All experimental data—osmotic pressures determined with different types of osmometers, light scattering data, and vapor pressure data at various concentrations—are listed in Tables II–IV, respectively. All the data from osmometry and light scattering are shown on a double-logarithmic plot of π/C vs. C in Figure 4. Agreement between the values of π/C obtained by osmometry and light scattering is satisfactory. The figure shows that π/C becomes independent of molecular weight at high concentrations.

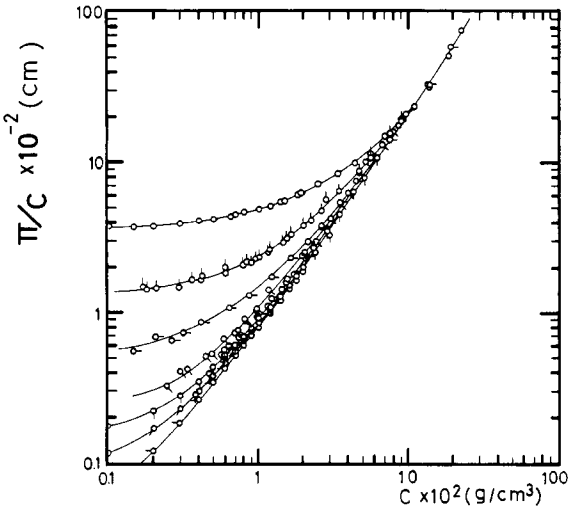

Figure 4. Osmotic pressures of poly(α-methylstyrenes) in toluene at 25 °C. The symbols ○, ◇, ▽, ▢, ▽, ⌀, and ⊖ denote data for α-104, α-12, α-103, α-110, α-112, α-113, and α-111, respectively. The data for α-112 were obtained by both osmotic pressure and light scattering measurements, and the data for α-113 and α-111 were obtained by light scattering measurements.

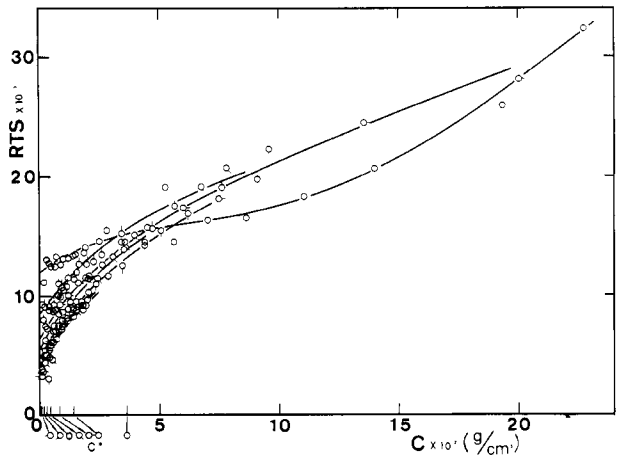

Figure 5. Apparent second virial coefficients of poly(α-methylstyrenes) in toluene at 25 °C. The symbols are the same as in Figure 4. C^* denotes the critical concentration for each sample.

To study the thermodynamic properties of polymer solutions at finite concentrations in more detail, it is convenient to define[11] an apparent second virial coefficient S by the following relationship:

$$RTS = (\pi/C - RT/M_n)/C \tag{6}$$

All experimental values of S evaluated from the data in Tables II and III are plotted against polymer concentration C in Figure 5. The concentration dependence of the lowest molecular weight polymer, α-104, is somewhat different from the others, though such an abnormality cannot be noticed in Figure 4. This slightly abnormal behavior may be caused by the different tacticity of this sample.[1,5]

It can be pointed out in Figure 5 that S depends on molecular weight and the values for high molecular weight samples are smaller than those for low molecular weight samples.

In the following discussion section, we examine the theories so far presented for moderately concentrated solutions, using the present experimental data. For that purpose, we need numerical values of thermodynamic interaction parameters. The thermodynamic properties of

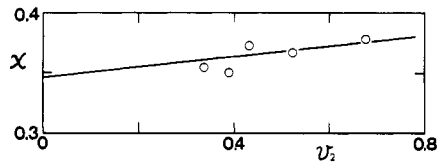

Figure 6. Polymer volume fraction dependence of the thermodynamic interaction parameter χ. The line denotes eq 12.

concentrated polymer solutions can well be expressed by the theory of Flory and Huggins.[3] In their theory, the osmotic pressure is given by

$$\pi = -RT/\bar{V}_1^\circ[\ln(1 - v_2) + (1 - 1/x)v_2 + \chi v_2^2] \quad (7)$$

where x is the molar volume ratio of polymer to solvent and χ is the thermodynamic interaction parameter. Thus, the χ parameter at each concentration can be evaluated from the experimental values of π as[7]

$$\chi = -\frac{\pi V_1^\circ}{RTv_2^2} + \frac{1}{xv_2} + \frac{1}{2} + \frac{v_2}{3} + \ldots \quad (8)$$

Although χ depends strongly on molecular weight not only in dilute solutions but also in moderately concentrated solutions, the χ parameter appears to approach a limiting relationship $\chi = \chi_1 + \chi_2 v_2$ if the concentrations are much higher than v_2^*.

The χ_1 parameter is related to the excluded-volume parameter z as follows:[12]

$$z = (3/2\pi)^{3/2}B(6\langle s^2\rangle_0/M)^{-3/2}M^{1/2} \quad (9)$$

and

$$B = (\bar{v}^2/V_1^\circ N_A)(1 - 2\chi_1) \quad (10)$$

where $\langle s^2\rangle_0$ is the unperturbed square radius of gyration. From light scattering measurements of poly(α-methylstyrene) in toluene at 25 °C, we had[1]

$$z = 3.45 \times 10^2 M^{1/2} \quad (11)$$

Introducing $\bar{v} = 0.837$ cm^3/g[6] and $\langle s^2\rangle_0/M = 8.25 \times 10^{-18}$[1,5] into eq 9 and 10 and comparing the result with eq 11, we find $\chi_1 = 0.346$. The solid line in Figure 6 is drawn with this value of intercept:

$$\chi = 0.346 + 0.44v_2 \quad (12)$$

Discussion

In dilute solutions, the osmotic pressure can be expressed in the form of a virial expansion. If truncated at the first order of concentration, the reduced osmotic pressure $\pi M/CRT$ is given by

$$\pi M/CRT = 1 + A_2MC \quad (13)$$

where the second virial coefficient A_2 is

$$A_2 = 4\pi^{3/2}N_A\bar{z}h(\bar{z})\frac{\langle s^2\rangle^{3/2}}{M^2} \quad (14)$$

and $\bar{z}h(\bar{z})$ is the penetration function. In good solvents, $\bar{z}h(\bar{z})$ is almost a constant (=0.2$_1$) independent of molecular weight, and polymer coils appear to behave like hard spheres in the intermolecular interaction.[1,2] From eq 1, 13, and 14, we have

$$\pi M/CRT = 1 + 1.12(C/C^*) \quad (15)$$

where C/C^* is the reduced concentration showing the degree of coil overlapping.

In the virial expansion, moreover, the apparent second virial coefficient S is given by

$$S = A_2 + A_3C + \ldots$$

$$S = A_2 + gA_2^2MC + \ldots \quad (16)$$

where A_3 is the third virial coefficient and g is a numerical constant, $g = A_3/A_2^2M$. Thus, if we truncate the expansion at the third virial coefficient and assume $g = 1/4$, S can be rewritten in terms of C/C^*

$$S/A_2 = 1 + 0.28(C/C^*) \quad (17)$$

$g = 1/4$ is assumed in the square root plot of osmotic pressure, i.e., in the plot of $(\pi/C)^{1/2}$ vs. C.[3]

Various theories have so far been presented to explain the thermodynamic properties of moderately concentrated solutions. Here, we refer to the theories of Fixman,[11,13,14] Yamakawa,[15] and Koningsveld et al.[16] and also a new theory of des Cloizeaux.[17,18]

(1) From analogy to critical phenomena, des Cloizeaux[17,18] concluded that the osmotic pressure obeys a scaling law of the following functional form:

$$\pi/C_pRT = F(C_pM^{3\nu}) \quad (18)$$

where C_p is the molar concentration of polymer, i.e., $C_p = C/M$, and ν is the excluded-volume exponent defined in the relationship between $\langle s^2\rangle$ and M at infinite dilution, that is, in $\langle s^2\rangle^{1/2} \propto M^\nu$. In good solvents ν is equal to $3/5$ according to the α^5 theory of Flory.[3]

Introducing the critical concentration into eq 18, we have

$$\pi M/CRT = F(C\langle s^2\rangle^{3/2}/M) = F(C/C^*) \quad (19)$$

That is, $\pi M/CRT$ is expressed as a function of C/C^*, which is the reduced concentration or the degree of coil overlapping. According to des Cloizeaux,[17,18] this function in moderately concentrated solutions is given by

$$F(C/C^*) = K'(C/C^*)^{1/(3\nu-1)} \quad (20)$$

where K' is a constant. Thus, we have

$$\pi M/CRT = K'(C/C^*)^{1/(3\nu-1)} \quad (21)$$

The apparent second virial coefficient S in moderately concentrated solutions, moreover, can be written as

$$S \propto (C/C^*)^{1/(3\nu-1)}/(MC) \quad (22)$$

if the molecular weight is high. Combining eq 22 with eq 1 and 14 and assuming that $\bar{z}h(\bar{z})$ is constant,[1] we have

$$S/A_2 = K''(C/C^*)^{-(3\nu-2)/(3\nu-1)} \quad (23)$$

where K'' is a constant.

The experimental relationship between $\langle s^2\rangle$ and M for poly(α-methylstyrene) in toluene is given by[1,19]

$$\langle s^2\rangle = 1.78 \times 10^{-18}M^{1.17} \quad (24)$$

Thus, the experimental value of ν is equal to 0.585, which is slightly lower than 0.6.[1,19] We remark that ν is predicted to be 0.588 by renormalization group theory.[20] Introducing this experimental value into eq 21 and 23 we have

$$\pi M/CRT = K'(C/C^*)^{1.32_5} \quad (25)$$

$$S/A_2 = K''(C/C^*)^{0.32_5} \quad (26)$$

Here, it should be noted that the scaling theory of des Cloizeaux does not predict the values of K' and K''.

A remarkable feature in the theory of des Cloizeaux[17,18] is that $\pi M/CRT$ or S/A_2 is given as a function of C/C^* only, irrespective of molecular weight. In contrast to the theory of des Cloizeaux, the older theories of Fixman,[11,13,14] Yamakawa,[15] and Koningsveld et al.[16] predict that $\pi M/$

Table II
Data of Osmotic Pressure of Poly(α-methylstyrenes) in Toluene at 25 °C

$C \times 10^2$, g/cm³	C/C^*	π, g/cm²	$\pi M/CRT$	$RTS \times 10^{-4}$	type of osmometer[a]
		A. α-104			
0.100_1	0.027_5	0.37_9	1.06_1	(2.17_7)	ZM (S)
0.148_8	0.040_9	0.55_2	1.03_9	0.92_7	ZM (S)
0.200_0	0.054_9	0.75_9	1.06_2	1.11_5	ZM (S)
0.300_4	0.082_5	1.19_0	1.11_0	1.30_4	ZM (S)
0.400	0.110	1.63_6	1.14_3	1.27_2	ZM (S)
0.500	0.137	2.01_3	1.17_6	1.25_4	ZM (S)
0.645	0.177	2.82_5	1.22_6	1.24_9	ZM (S)
0.698	0.192	3.14_5	1.26_1	1.33_6	ZM (S)
0.898	0.247	4.23_2	1.31_8	1.26_4	ZM (S)
1.002	0.275	4.89_4	1.36_8	1.31_2	ZM (S)
1.200	0.330	6.19_1	1.444	1.322	ZM (S)
1.397	0.384	7.61_0	1.525	1.341	ZM (S)
1.499	0.412	8.36_1	1.562	1.338	ZM (S)
1.837	0.505	11.17_8	1.703	1.367	ZM (S)
1.902	0.523	11.89_9	1.751	1.411	ZM (S)
2.506	0.688	18.14_9	2.027	1.464	ZM (S)
		18.23	2.037	1.477	ZM (D)
3.407	0.936	28.93	2.377	1.444	ZM (D)
4.419	1.21_4	44.18	2.799	1.451	ZM (D)
5.608	1.54_1	65.55	3.272	1.447	ZM (D)
7.018	2.92_8	105.48	4.208	1.632	ZM (D)
8.604	2.36_4	153.2_0	4.985	1.654	ZM (D)
11.02	3.02_7	261.1	6.632	1.825	ZM (D)
		262.7	6.672	1.838	FD (D)
13.96	3.83_5	438.9	8.799	1.994	ZM (D)
		466.1	9.344	2.134	FD (D)
18.63	5.11_8	965.9	14.52	2.592	FD (D)
22.76	6.25_3	1753.5	21.57	3.227	FD (D)
		B. α-12			
0.170_2	0.122	0.25_4	1.20_6	(1.33_3)	ZM (S)
0.180_0	0.129	0.25_4	1.13_9	0.80_5	ZM (S)
0.207_5	0.148	0.30_3	1.17_8	0.92_5	HM
0.291_3	0.208	0.43_3	1.19_9	0.74_8	HM
0.359_0	0.257	0.59_6	1.33_9	1.09_1	ZM (S)
0.410_5	0.294	0.67_4	1.32_5	0.91_1	HM
0.421_6	0.302	0.73_4	1.40_4	1.11_9	ZM (S)
0.591_3	0.423	1.05_6	1.44_1	0.87_6	HM
0.599_0	0.429	1.21_0	1.62_9	1.25_5	ZM (S)
0.600_7	0.430	1.09_8	1.47_5	0.93_2	HM
0.794_5	0.568	1.64_3	1.66_8	1.00_6	HM
0.838_0	0.599	1.83_7	1.76_8	1.10_2	ZM (S)
0.891_9	0.638	1.92_2	1.73_8	0.99_4	HM
0.951_1	0.680	2.17_9	1.84_8	1.07_5	ZM (S)
1.012_5	0.724	2.36_1	1.88_1	1.05_0	HM
1.168	0.835	2.75_5	2.04_1	1.08_0	HM
1.197	0.856	3.17_6	2.14_0	1.15_7	ZM (S)
1.463	1.04_6	4.30_3	2.37_2	1.14_3	HM
1.557	1.11_4	4.89_3	2.53_4	1.20_3	ZM (S)
1.651	1.18_1	5.55_4	2.713	1.269	ZM (S)
2.001	1.43_1	7.61_4	3.069	1.267	ZM (S)
2.244	1.60_5	9.34_6	3.359	1.291	ZM (S)
2.612	1.86_8	12.54_3	3.873	1.352	ZM (S)
2.803	2.00_5	15.84_4	4.559	1.564	ZM (S)
		15.80	4.546	1.558	ZM (D)
3.436	2.45_8	22.44_7	5.269	1.532	ZM (D)
4.724	3.37_9	41.64	7.109	1.597	ZM (D)
		40.0	6.829	1.523	FD (D)
5.621	4.02_1	60.90	8.739	1.701	ZM (D)
		64.0	9.184	1.797	FD (D)
7.649	5.47_1	120.85	12.74_4	1.899	ZM (D)
		122.0	12.86_4	1.919	FD (D)
9.090	6.50_2	176.88	15.69_7	2.001	ZM (D)
		172.0	15.26_9	1.94_3	FD (D)
		C. α-103			
0.148_5	0.180	0.08_2	1.1_1	0.36_4	ZM (S)
0.205_1	0.245	0.14_2	1.3_9	0.94_6	ZM (S)
0.261_8	0.318	0.16_8	1.2_9	0.54_6	ZM (S)
0.318_3	0.387	0.23_3	1.4_7	0.72_9	ZM (S)
0.410_5	0.499	0.35_4	1.7_3	0.88_4	ZM (S)
0.637_4	0.775	0.67_8	2.12_9	0.88_5	ZM (S)
0.861_2	1.04_6	1.11_9	2.60_1	0.92_9	ZM (S)
1.219	1.48_1	2.10_2	3.45_1	1.00_5	ZM (S)

Table II (*Continued*)

$C \times 10^2$, g/cm³	C/C^*	π, g/cm²	$\pi M/CRT$	$RTS \times 10^{-4}$	type of osmometer[a]
1.622	1.97_0	3.75_1	4.62_7	1.11_8	ZM (S)
2.112	2.56_6	6.31_5	5.98_2	1.179	ZM (S)
2.602	3.16_1	9.83_7	7.56_3	1.260	ZM (S)
		9.94	7.64_3	1.276	ZM (D)
3.508	4.26_2	18.64	10.63	1.371	ZM (S)
		19.23	10.97	1.419	ZM (D)
4.501	5.46_9	34.17	15.19	1.575	ZM (D)
5.994	7.28_3	65.36	21.82	1.736	ZM (D)
7.494	9.10_6	105.5	28.17	1.812	ZM (D)
13.542	16.45	454.9	67.21	2.443	FD (D)
20.01	24.31	1133.7	113.32	2.805	FD (D)
		D. α-110			
0.242_6	0.567	0.07_8	1.5_2	0.44_9	HM
0.299_2	0.699	0.12_1	1.9_0	0.63_8	HM
0.333_5	0.779	0.14_0	1.9_6	0.61_2	HM
0.383_8	0.897	0.15_2	1.8_6	0.47_5	HM
0.442_4	1.03_4	0.22_5	2.4_0	0.66_9	HM
0.490_1	1.14_6	0.25_9	2.4_8	0.64_3	HM
0.518_1	1.21_1	0.23_8	2.1_6	0.47_5	HM
0.584_5	1.36_6	0.38_9	3.1_3	0.77_5	HM
0.684_6	1.60_1	0.50_2	3.4_5	0.75_9	HM
0.726_1	1.69_7	0.55_2	3.5_8	0.75_3	HM
0.811_0	1.89_6	0.73_6	4.27_2	0.85_7	HM
0.817_5	1.91_1	0.67_6	3.88_9	0.75_0	HM
0.964_6	2.25_5	1.00_1	4.88_4	0.855	HM
0.968_5	2.26_4	1.03_1	5.00_6	0.879	HM
1.229	2.87_3	1.61_2	6.17_4	0.895	HM
1.234	2.88_5	1.52_3	5.80_6	0.827	HM
1.283	2.99_9	1.83_4	6.72_8	0.949	HM
1.541	3.60_3	2.43_8	7.44_4	0.890	HM
1.542	3.60_5	2.61_1	7.96_6	0.958	HM
1.969	4.60_3	4.74_5	11.34	1.115	HM
2.046	4.78_4	5.23_8	12.05	1.148	HM
2.428	5.67_7	7.28_4	14.11	1.148	HM
3.047	7.12_4	12.96_5	20.02	1.328	HM
3.572	8.34_6	19.23_2	25.33	1.449	HM
3.984	9.30_8	24.75_6	29.24	1.507	HM
5.243	12.25	53.58_3	48.09	1.909	HM
6.742	15.75	88.32_0	61.64	1.912	HM
7.783	18.19	126.62_9	96.56	2.064	HM
		E. α-112			
0.383_1	1.33	0.10_8	2.0_3	0.37_3	HM
0.474_3	1.65	0.18_7	2.8_2	0.53_3	HM
0.561_3	1.95	0.29_4	3.7_7	0.68_6	HM
0.591_2	2.05	0.33_3	4.0_5	0.71_7	HM
0.591_9	2.06	0.30_7	3.7_4	0.64_2	HM
0.626_8	2.18	0.37_6	4.3_2	0.73_5	HM
0.737_9	2.56	0.50_2	4.8_9	0.73_3	HM
0.979_2	3.40	0.92_0	6.7_6	0.81_8	HM
1.143	3.97	1.25_7	7.9_2	0.84_1	HM
1.425	4.95	2.05_2	10.36	0.91_3	HM
1.716	5.96	3.08_9	12.95	0.967	HM
2.056	7.14	4.68_8	16.41	1.041	HM
2.340	8.13	6.38_9	19.65	1.107	HM
2.883	10.0_1	10.14_8	25.33	1.173	HM
3.496	12.1_3	15.93_9	32.82	1.265	HM
4.393	12.2_5	28.03	45.91	1.421	HM
5.086	17.6_6	40.53	57.36	1.540	HM
6.226	21.6_2	66.56	76.93	1.695	HM
9.542	33.1_3	203.91	153.79	2.223	HM

[a] S and D denote the static and dynamic methods, respectively.

CRT or S/A_2 is not a function of C/C^* only, as discussed in the following.

(2) Fixman[11,13,14] developed a theory of osmotic pressure and dimensions of polymer coil in moderately concentrated solutions by applying the variation method to the Born–Green–Kirkwood equation based on the assumption of the Gaussian intermolecular potential of Flory and Krigbaum.[3] The apparent second virial coefficient S and the expansion factor α_c at finite concentrations, which is defined by the ratio of the radius of gyration at finite concentrations $\langle s^2\rangle_c^{1/2}$ to the unperturbed radius of gyration $\langle s^2\rangle_0^{1/2}$, are given, respectively, by

$$S = 2\pi A_0 \alpha^3 B'^{-3/2} M^{-2} N_A [1 - (1 + \delta)^{-5/2}] \quad (27)$$

$$\alpha_c^2 - 1 = 0.1777A\left[1 - 15.87 \int_{\delta(A,0)}^{\delta(A,\gamma)} I(\delta)\, d\delta\right] \quad (28)$$

where $I(\delta)$ is a function of δ, which is a function of A and γ. Moreover

$$A_0 = 7.18z/\alpha^3 = 7.18\bar{z} \qquad A = 7.18z/\alpha_c^3$$
$$B' = 9.61/(6\langle s^2\rangle_0) \qquad \gamma = \gamma'\alpha_c^3 \qquad (29)$$
$$\gamma' = \pi^{3/2}B'^{3/2}\rho$$

where ρ is the number density of polymer and γ' is the dimensionless measure of concentration. Combining eq 27 with eq 1, 6, and 14 we can express $\pi M/CRT$ or S/A_2 in terms of C/C^* as

$$\pi M/CRT = 1 + 3\pi^{1/2}\bar{z}[1 - (1 + \delta)^{-5/2}](C/C^*) \quad (30)$$

$$S/A_2 = [1 - (1 + \delta)^{-5/2}]/h(\bar{z}) \quad (31)$$

where δ is a function of C/C^* and $\bar{z}$. Apparently, $\pi M/CRT$ or S/A_2 is a function of not only C/C^* but also an excluded-volume parameter $\bar{z}$. If the concentration of polymer C, the molecular weight M, the expansion factor α, the excluded-volume parameter $\bar{z}$, and the unperturbed square radius of gyration $\langle s^2\rangle_0$ are given,[1] we can calculate the theoretical value of S or π.

(3) Using the random flight model, Yamakawa[15] derived theoretical equations for the apparent second virial coefficient S and the expansion factor at finite concentrations α_c by solving a differential equation derived from the Kirkwood integral equation with use of a coupling parameter method as follows:

$$S = 4\pi^{3/2}N_A\frac{\langle s^2\rangle^{3/2}}{M^2}\bar{z}H(C,\bar{z}_c) \quad (32)$$

and

$$\alpha_c = \alpha \exp\left[-C\left(4\pi^{3/2}N_A\frac{\langle s^2\rangle^{3/2}}{M}\bar{z}\right)(\kappa/k_1)\phi_z(\bar{z})\right] \quad (33)$$

with

$$H(C,\bar{z}) = \exp\left[-k_1\bar{z}_c + C\left(8\pi^{3/2}N_A\frac{\langle s^2\rangle^{3/2}}{M}\bar{z}\right)\phi_1(\bar{z}_c)\right] + \phi_2(\bar{z}_c) + C\left(8\pi^{3/2}N_A\frac{\langle s^2\rangle^{3/2}}{M}\bar{z}\right)\phi_3(\bar{z}) \quad (34)$$

where

$$\phi_1(\bar{z}_c) = [1 - \exp(-\lambda_1\bar{z}_c)][1 - \exp(k_1\bar{z}_c)]/(k_1\bar{z}_c)$$
$$\phi_2(\bar{z}_c) = 1 - [1 - \exp(-k_1\bar{z}_c)]/(k_1\bar{z}_c) \quad (35)$$
$$\phi_3(\bar{z}_c) = [\exp(-k_1\bar{z}_c)][\sinh(k_1\bar{z}_c) - k_1\bar{z}_c]/(k_1\bar{z}_c)^2$$
$$\bar{z}_c = z/\alpha_c^3 \qquad \bar{z} = z/\alpha^3$$

and the constants k_1, λ_1, and κ have values of 5.731, 1.664, and 0.4552, respectively. Combining eq 32 with eq 1, 6, and 14, we can rewrite $\pi M/CRT$ or S/A_2 in terms of C/C^* as

$$\pi M/CRT = 1 + 3\pi^{1/2}\bar{z}H(C,\bar{z}_c)(C/C^*) \quad (36)$$

$$S/A_2 = H(C,\bar{z}_c)/h(\bar{z}) \quad (37)$$

where $H(C,\bar{z}_c)$ is a function of C/C^* and $\bar{z}_c$. Thus, $\pi M/CRT$ or S/A_2 is a function of not only C/C^* but also excluded-volume parameters $\bar{z}$ and $\bar{z}_c$. The theoretical value of S or π is calculated if C, M, α, z, and $\langle s^2\rangle_0$ are given.[1]

(4) Koningsveld et al.[16] presented a theory of polymer solution applicable to a wide range of concentration. In their theory the interaction parameter χ is assumed to consist of two terms, one which represents the segment–segment interaction in concentrated solution and the other

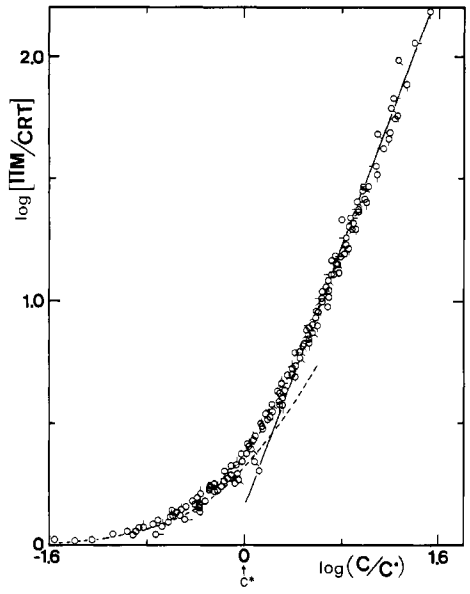

Figure 7. Double-logarithmic plots of reduced osmotic pressure and reduced concentration obtained from the experimental data. The symbols are the same as in Figure 4. The full line and the broken curve denote eq 25 and 15, respectively.

which shows the intermolecular excluded-volume effect of polymer coils. Their result is

$$S = (\bar{v}^2/\bar{V}_1^\circ)(\tfrac{1}{2} - \chi) + (\bar{v}^3/\bar{V}_1^\circ)C/3 + (\bar{v}^4/\bar{V}_1^\circ)C_2/4 + \ldots \quad (38)$$

$$\chi = \chi_1 + \chi_2\bar{v}C + g^*[1 + \lambda - \lambda_c C]e^{-\lambda_c C} \quad (39)$$

where

$$\lambda_c = (4\pi/3)N_A\langle s^2\rangle^{3/2}/M \qquad \lambda = \lambda_c/\bar{v}$$

and

$$g^* = [(\tfrac{1}{2} - \chi_1)/(1 + \lambda)][1 - (\bar{V}_1^0/\bar{v}^2)A_2/(\tfrac{1}{2} - \chi_1)] \quad (40)$$

Here, we may use our experimental result, eq 12, for the χ_1 and χ_2 parameters in eq 39. It is clear that $\pi M/CRT$ or S/A_2 is a function of not only C/C^* ($=\lambda_c C$) but also thermodynamic parameters such as χ_1, χ_2, and A_2. The theoretical value of S or π is calculated if C, M, $\langle s^2\rangle_0$, χ_1, and χ_2 are given.[1]

Now we will compare those four theories with the present data. Figure 7 shows the double-logarithmic plot of the experimental reduced osmotic pressure vs. the reduced concentration. It is clear from the figure that the reduced osmotic pressure is a function of the reduced concentration as predicted in the theory of des Cloizeaux.[17,18] The slope of the line at $C > C^*$ in the figure is 1.32_5, which is in good agreement with the scaling theory of des Cloizeaux[17,18] (eq 25). The proportional constant K' in eq 25 was experimentally found to be 1.5_0.

The broken curve in Figure 7 denotes the virial expanded form of osmotic pressure (eq 13). The calculated values agree with the data at concentrations lower than the critical one. The crossover point from dilute solution to moderate concentration is around $1.6C^*$, which is between C^* defined here and a critical concentration defined by $M/\langle s^2\rangle^{3/2}N_A$.

In Figure 8 the theory of Yamakawa[5] is expressed in the form of a $\pi M/CRT$ vs. C/C^* plot. No universal relationship is found between $\pi M/CRT$ and C/C^*. The situation is the same in all other theories of Fixman[11,13,14] and Koningsveld et al.[16] This result is understandable because $\pi M/CRT$ is a function of not only C/C^* but also ther-

Table III
Light Scattering Data of Poly(α-methylstyrenes) in Toluene at 25 °C

α-112		α-113		α-111	
C, g/dL	$(KC/R_\theta)_{\theta=0} \times 10^6$	C, g/dL	$(KC/R_\theta)_{\theta=0} \times 10^6$	C, g/dL	$(KC/R_\theta)_{\theta=0} \times 10^6$
0.060_1	0.70_0	0.052_4	0.46_0	0.033_5	0.20_3
1.108_1	0.86_5	0.104_9	0.68_0	0.052_4	0.27_1
0.205_7	1.40	0.196_7	1.15	0.097_0	0.43_6
0.304_8	2.00	0.288_2	1.68	0.142_7	0.640
0.366_7	2.43	0.392_2	2.25	0.194_5	0.941
0.573_2	3.88	0.523_9	3.45	0.288_1	1.52
0.864_0	6.25	0.563_6	3.88	0.391_3	2.19
1.158	8.8	0.794_7	5.75	0.530_8	3.32
1.520	12.3	0.967_5	7.45	0.744_6	4.84
1.994	17.5	1.243	9.85	0.932_6	6.50
2.376	21.5	1.894	16.8	1.203	8.88
2.842	28.0			1.448	11.56
3.859	41.7			1.956	16.40

Table IV
Vapor Pressure Data of
Poly(α-methylstyrene) α-112 in Toluene at 25 °C

C, g/mL	P, mmHg	P_0/P^a
0.367_4	28.09	1.035
0.421_0	27.63	1.052
0.466_5	27.23	1.066
0.565_6	25.82	1.125
0.728_1	21.93	1.324

[a] P_0 is the vapor pressure of toluene at 25 °C.

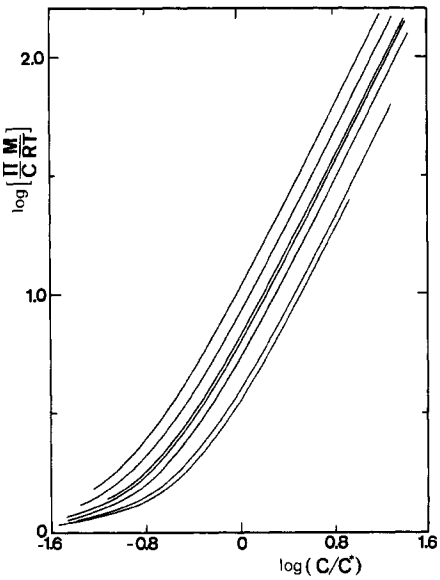

Figure 8. Double-logarithmic plots of reduced osmotic pressure and reduced concentration calculated from the theory of Yamakawa. The curves denote the theoretical ones calculated for α-111, α-113, α-112, α-110, α-103, α-12, and α-104 from top to bottom.

modynamic parameters in these theories.

In order to examine the theories in more detail, comparison of their theoretical apparent second virial coefficients with experimental data may be most promising. The experimental values of S/A_2 are plotted against C/C^* in Figure 9, where the experimental values of A_2 determined from light scattering and osmotic pressure measurements are used in calculating S/A_2 in both measurements. The values of A_2 in both measurements are slightly different because the contributions of the third virial coefficient are different in both measurements. The solid line in the region $C/C^* > 1$ in the figure shows scaling eq 26 with K'' = 1.25. The value of K'' (=1.25) chosen to have the best agreement between the experimental and calculated values

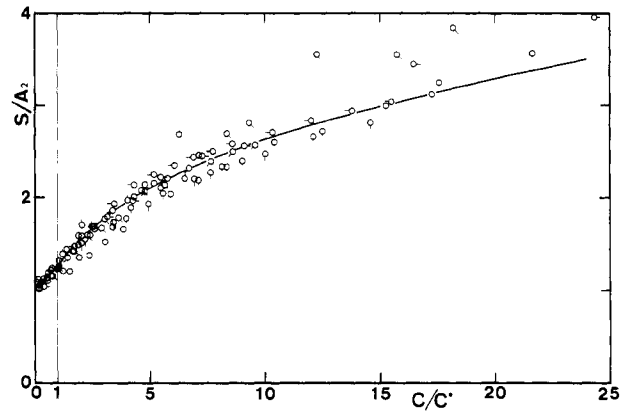

Figure 9. Plots of S/A_2 against C/C^*. The symbols are the same as in Figure 4. The curve denotes eq 26 with K'' = 1.25.

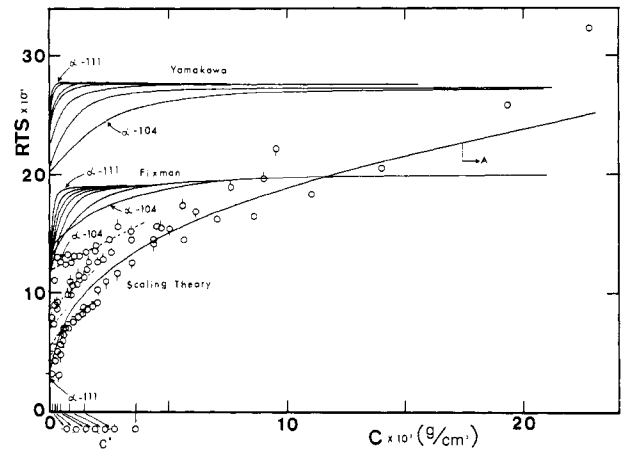

Figure 10. Comparison between apparent second virial coefficients calculated by the theories of Fixman, Yamakawa, and des Cloizeaux and typical experimental data. Theories of Fixman and Yamakawa: The curves denote the theoretical values for α-111, α-113, α-112, α-110, α-103, α-12, and α-104 from top to bottom. Scaling theory of des Cloizeaux: The full curve A denotes eq 26 with K'' = 1.25. The broken lines denote the calculated values from eq 17 in the region $C < C^*$ for α-104, α-12, α-103, α-110, α-112, α-113, and α-111 from top to bottom. The symbols are the same as in Figure 4. C^* denotes the critical concentration for each sample.

is very close to 1.28, which is obtained from eq 17 at C/C^* = 1. On the other hand, the theories of Fixman,[11,13,14] Yamakawa,[15] and Koningsveld et al.[16] do not predict the universal relationship between S/A_2 and C/C^* but predict different curves for different molecular weight samples.

To see the features of the scaling theory more clearly, the scaling theory is compared with typical experimental

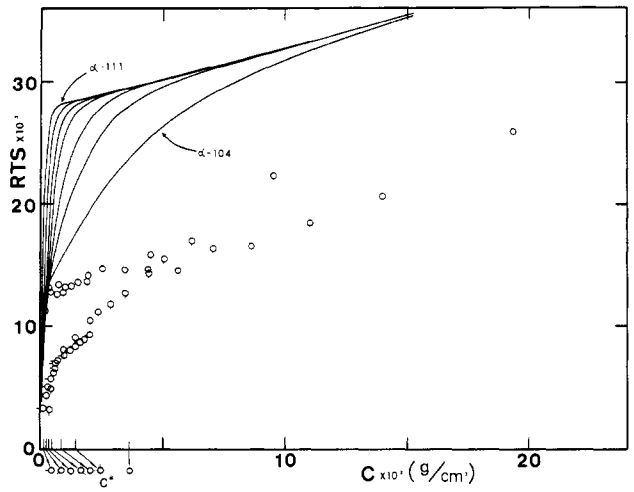

Figure 11. Comparison between apparent second virial coefficients calculated by the theory of Koningsveld et al. and typical experimental data. The curves denote the theoretical values for α-111, α-113, α-112, α-110, α-103, α-12, and α-104 from top to bottom. The symbols are the same as in Figure 4. C^* denotes the critical concentration for each sample.

data in the form of S vs. C in Figure 10. The full line denotes the calculated values of eq 26 with $K'' = 1.25$ and broken lines show the virial expansion theory, that is, the calculated values of eq 17. If the polymer concentration C is lower than C^*, the virial expansion theory is sufficient to explain the experimental data. Many experimental points are found in the region $C < C^*$ if the molecular weight is low. If the molecular weight is high, however, most experimental points in osmometry and light scattering are obtained in the region $C > C^*$. It is clear from Figures 9 and 10 that the experimental data of S in that region can well be explained by the scaling theory.

The theoretical S values of Fixman,[11,13,14] Yamakawa,[15] and Koningsveld et al.[16] are also shown in Figures 10 and 11. The main feature of those theories is that S for high molecular weight samples increases more rapidly than that for low molecular weight samples; that is, S for high molecular weight polymers is higher than S for low molecular weight polymers. The theoretical prediction is opposite to the experimental results, as can be observed in the figures.

In our opinion, the main difference between the older theories and the scaling theory is in the concentration region covered by the respective theories. In the scaling theory, data in the region $C > C^*$ are compared with the theory and it is assumed that the virial expansion theory is sufficient for the data in the region $C < C^*$. In the older theories, on the other hand, the virial expansion form of osmotic pressure is modified to explain the data which are mostly in the region $C < C^*$. If the concentration becomes higher than C^*, the theoretical S immediately levels off or follows the theory of Flory and Huggins.[3] The region which is called "the semidilute solution" in the scaling theory is not well-defined in the older theories.

In sum we conclude that the reduced osmotic pressure in both dilute and moderately concentrated solutions or semidilute solutions is a function of the reduced concentration or the degree of coil overlapping, irrespective of molecular weight and concentration, and the thermodynamic behavior of moderately concentrated solutions is entirely different from that of dilute solutions, as predicted in the scaling theory.

Acknowledgment. We thank Dr. T. Fujimoto for his cooperation in the measurement of vapor pressure and Mr. N. Ueno, Mr. M. Kawachi, and Mr. S. Ban for their help in the measurement of osmotic pressure. This work was supported in part by a Grant-in-Aid for Scientific Research from the Ministry of Education, Science and Culture of Japan.

References and Notes

(1) Kato, T.; Miyaso, K.; Noda, I.; Fujimoto, T.; Nagasawa, M. *Macromolecules* **1970**, *3*, 777.
(2) Noda, I.; Kitano, T.; Nagasawa, M. *J. Polym. Sci., Polym. Phys. Ed.* **1977**, *15*, 1129.
(3) Flory, P. J. "Principles of Polymer Chemistry"; Cornell University Press: Ithaca, N.Y., 1953.
(4) Graessley, W. W. *Adv. Polym. Sci.* **1974**, *16*, 1.
(5) Noda, I.; Mizutani, K.; Kato, T.; Fujimoto, T.; Nagasawa, M. *Macromolecules* **1970**, *3*, 787.
(6) Noda, I.; Mizutani, K.; Kato, T. *Macromolecules* **1977**, *10*, 618.
(7) Flory, P. J.; Daoust, H. *J. Polym. Sci.* **1957**, *25*, 429.
(8) Zimm, B. H.; Myerson, I. *J. Am. Chem. Soc.* **1946**, *68*, 911.
(9) Kawai, T.; Inoue, Y. *Kobunshi Jikkengaku Koza* **1957**, *6*, 67.
(10) Saito, N. "Introduction to Polymer Physics", Rev. ed.; Shokabo: Tokyo, 1967.
(11) Fixman, M. *J. Chem. Phys.* **1960**, *33*, 370.
(12) Yamakawa, H. "Modern Theory of Polymer Solutions"; Harper and Row: New York, 1971.
(13) Fixman, M. *Ann. N.Y. Acad. Sci.* **1961**, *89*, 654.
(14) Fixman, M. *J. Polym. Sci.* **1960**, *47*, 91.
(15) Yamakawa, H. *J. Chem. Phys.* **1965**, *43*, 1334.
(16) Koningsveld, R.; Stockmayer, W. H.; Kennedy, J. W.; Keleintjens, L. A. *Macromolecules* **1974**, *7*, 73.
(17) des Cloizeaux, J. *J. Phys. (Paris)* **1975**, *36*, 1199.
(18) Daoud, M.; Cotton, J. P.; Farnoux, B.; Jannink, G.; Sarma, G.; Benoit, J.; Duplessix, C.; Picot, C.; de Gennes, P. G. *Macromolecules* **1975**, *8*, 804.
(19) Mijnlieff, P. F.; Wiegel, F. W. *J. Polym. Sci., Polym. Phys. Ed.* **1978**, *16*, 245.
(20) Le Guillou, J. C.; Zinn-Justin, J. *Phys. Rev. Lett.* **1977**, *39*, 95.